JBC Papers in Press. Published on April 4, 2018 as Manuscript RA118.002175
The latest version is at http://www.jbc.org/cgi/doi/10.1074/jbc.RA118.002175

Activation of stimulator of interferon genes (STING) induces ADAM17-mediated shedding of the immune semaphorin SEMA4D

Kou Motani[1*] and Hidetaka Kosako[1]

From the [1]Division of Cell Signaling, Fujii Memorial Institute of Medical Sciences, Tokushima University, 3-18-15 Kuramoto-cho, Tokushima 770-8503, Japan

Running title: *SEMA4D shedding by STING*

[*]To whom correspondence should be addressed: Kou Motani: Division of Cell Signaling, Fujii Memorial Institute of Medical Sciences, Tokushima University, 3-18-15 Kuramoto-cho, Tokushima 770-8503, Japan; motani@tokushima-u.ac.jp; Tel. 81-88-634-6411; Fax. 81-88-634-6405

Keywords: ADAM, cell surface protein, inflammation, proteomics, post-translational modification, STING, SEMA4D

ABSTRACT

Stimulator of interferon genes (STING) is an endoplasmic reticulum (ER)-resident membrane protein that mediates cytosolic pathogen DNA–induced innate immunity and inflammatory responses in host defenses. STING is activated by cyclic di-nucleotides and is then translocated to the Golgi apparatus, an event that triggers STING assembly with the downstream enzyme TANK-binding kinase 1 (TBK1). This assembly leads to the phosphorylation of the transcription factor interferon regulatory factor 3 (IRF3), which, in turn, induces expression of type-I interferon (IFN) and chemokine genes. STING also mediates inflammatory responses independently of IRF3, but these molecular pathways are largely unexplored. Here, we analyzed the RAW264.7 macrophage secretome to comprehensively identify proinflammatory factors released into the extracellular medium upon STING activation. In total, we identified 1,299 proteins in macrophage culture supernatants, of which 23 were significantly increased after STING activation. These proteins included IRF3-dependent cytokines, as well as previously unknown targets of STING, such as the immune semaphorin SEMA4D/CD100, which possesses proinflammatory cytokine-like activities. Unlike for canonical cytokines, the expression of the SEMA4D gene was not up-regulated. Instead, upon STING activation, membrane-bound SEMA4D was cleaved into a soluble form, suggesting the presence of a post-translational shedding machinery. Importantly, the SEMA4D

shedding was blocked by TMI-1, an inhibitor of the sheddase ADAM metallopeptidase domain 17 (ADAM17), but not by the TBK1 inhibitor BX795. These results suggest that STING activates ADAM17 and that his activation produces soluble proinflammatory SEMA4D independently of the TBK1/IRF3-mediated transcriptional pathway.

Introduction

The detection of cytosolic DNAs derived from various pathogens triggers innate immune and inflammatory responses, which are essential for host defense (1). In contrast, endogenous self-DNA does not induce an immune response normally, because it is localized to the nucleus or mitochondria. However, inadequate accumulation of self-DNA in cytoplasm can also activate innate immunity (2). During animal development, tissue turnover and definitive erythropoiesis, apoptotic cells and pyrenocytes are engulfed by macrophages (3,4) and their DNA is degraded by the lysosomal enzyme DNaseII. If this degradation machinery is impaired in macrophages, accumulated apoptotic or pyrenocyte DNA leaks from the lysosome into the cytoplasm and triggers a strong inflammatory response, leading to severe anemia and polyarthritis (5-9). Of note, loss-of-function mutations in DNaseII have been recently identified in patients with autoinflammation featuring severe neonatal anemia and deforming arthropathy (10). Understanding immune response triggered by cytoplasmic DNA is an important issue to resolve inflammatory diseases.

STING is an ER-resident transmembrane protein that is essential for DNA-induced innate immune signaling (11). STING is activated by binding to cyclic di-nucleotides such as cyclic GMP-AMP (cGAMP) which is produced as an intracellular second messenger when cGAMP synthase (cGAS) recognizes cytosolic DNA (12-15). Upon binding to cGAMP, STING causes its dimerization and translocation from the ER to the Golgi apparatus (16-18). After relocation, STING recruits a serine/threonine kinase TBK1, leading to the phosphorylation of IRF3 and upregulation of type-I IFN and IFN-stimulated genes (ISG) including IFN-β and CXCL10 (19,20).

IFN-β production via STING-TBK1-IRF3 axis is crucial for development of anemia in DNaseII deficient mice (21). However, another phenotype polyarthritis is dependent of STING but not IRF3 (21). Similarly, systemic inflammation characterized by interstitial lung disease, skin lesions and hypercytokinemia in patients with activating mutations of STING gene has been shown to be IRF3-independent using a mouse model (22). These observations suggest that additional signaling pathway(s) is induced downstream of STING. Importantly, lack of proinflammatory cytokine genes such as TNF-α, IL-6 or IL-1β inhibited arthritis of the DNaseII-null mice (8). Although STING activates another transcriptional factor NF-κB which induces the proinflammatory cytokine gene expression, this activation is rather weak (11,23,24). Thus, it is unclear whether NF-κB-mediated gene activation is sufficient for STING-mediated inflammatory response.

Here, we performed unbiased comprehensive secretome analysis and identified that activation of STING promoted the cleavage of plasma membrane protein SEMA4D to release the inflammatory soluble form without its gene induction. We also found that TNF-α protein was dramatically increased in culture supernatant of STING-activated cells, although its mRNA expression was moderately induced in this

condition. The production of soluble SEMA4D as well as TNF-α were completely blocked by an inhibitor of ADAM17 sheddase. On the other hand, the treatment of cycloheximide (CHX) or TBK1 inhibitor did not abrogate the shedding of SEMA4D. These results suggest that STING activates ADAM17-mediated post-translational shedding machinery. Because soluble SEMA4D is known to activate inflammatory cytokine production, the STING-ADAM17-SEMA4D axis may be required for optimal inflammatory response.

Results

Identification of SEMA4D as a novel protein released by STING agonist

To determine the inflammatory factors released from STING-activated cells, we prepared culture supernatants from Raw264.7 murine macrophage cells treated with or without DMXAA, a cell-permeable synthetic STING agonist. Like a natural ligand, DMXAA directly binds to murine STING and causes its conformational activation (15). The DMXAA-treated cells were cultured for 4 h under the serum-free condition to prevent contamination of serum-derived abundant proteins, but no significant cell death was observed at least during the 4-h incubation (data not shown). After collection of proteins from the conditioned medium, we performed an unbiased proteomic analysis by shotgun LC-MS/MS (Fig. 1A). In total, we identified 1,299 proteins, of which 23 proteins are significantly increased ($P < 0.01$, fold-increase > 4) by DMXAA stimulation (Fig. 1B, Table 1 and Table S1). These successfully included IRF3-dependent cytokines such as IFN-β and CXCL10, and the most increased protein was TNF-α (about 150-fold increase). We also identified novel downstream targets of STING including SEMA4D, LRPAP1 and Fam3C. To confirm these results, we performed targeted LC-MS/MS analysis using parallel reaction monitoring (PRM) which enables highly specific and accurate protein quantification of multiple proteins simultaneously (25). As expected, the protein levels of SEMA4D, LRPAP1 and Fam3C in culture supernatants were increased about 3 to 6 fold by DMXAA (Fig. 1C and Table S2). DMXAA did not induce release of other class 4 semaphorin member SEMA4B or chemokine CCL9 (Fig. 1C and Table S2), confirming that specific set of proteins were released by stimulation with the STING agonist. Among identified 23 proteins, SEMA4D has been well characterized as a proinflammatory protein (26). Notably, the number of peptide spectrum matches (PSMs) of SEMA4D was relatively high among them (Table 1), suggesting that SEMA4D is an abundant protein in culture supernatant of the STING-activated cells. Thus, the activation of STING causes the release of the inflammatory factor SEMA4D in addition to known cytokines.

STING induces SEMA4D shedding independent of gene expression

To further confirm the STING-mediated release of SEMA4D, we performed Western blotting analysis of culture supernatant using antibody recognizing extracellular domain of SEMA4D. As shown in Fig. 2A, we could detect SEMA4D release 2 and 4 h after DMXAA stimulation. To determine whether STING is essential for DMXAA-induced release of SEMA4D, Raw264.7 cells lacking STING were generated using the CRISPR/Cas9 system. We confirmed again that SEMA4D was released along with TBK1 activation in DMXAA-stimulated wild-

type (WT) cells (Fig. 2B). In contrast, neither SEMA4D release nor TBK1 activation was observed in STING-deficient cells and this phenotype was rescued by ectopic expression of STING (Fig. 2B). Because STING activates transcription of type I interferon and inflammatory cytokine genes, we checked the induction of the SEMA4D gene after DMXAA stimulation. Real-time PCR analysis showed that DMXAA did not induce the expression of SEMA4D mRNA (Fig. 3A). As a control, we examined the expression levels of canonical cytokine genes and the IFN-β and CXCL10 mRNAs were dramatically increased about 500 to 1,500 fold after DMXAA stimulation (Fig. 3A). The expression of TNF-α mRNA was also up-regulated but only 8-fold increase although the protein level in the cell medium was increased about 150 fold, which is comparable to IFN-β and CXCL10 (Fig. 1C and Fig. 3A). These observations prompted us to speculate that STING activates not only transcription but also post-translational machinery to release SEMA4D and TNF-α. To confirm this possibility, the cells were treated with CHX to inhibit *de novo* protein synthesis, and then stimulated with DMXAA. As expected, production of CXCL10 was blocked by treatment of CHX in a dose-dependent manner, whereas SEMA4D was still released even in the presence of high-dose CHX (Fig. 3B). Because SEMA4D is a plasma membrane protein and its soluble ectodomain is generated by proteolytic cleavage (26), we tested whether STING agonist promotes shedding of SEMA4D. The total cell lysates and culture supernatants were prepared at the same time and the cleavage was analyzed by Western blotting. As shown in Fig. 3C, the full length membrane form of SEMA4D was reduced by DMXAA treatment in the cell lysates, concomitant with an increase of cleaved form of SEMA4D in the culture supernatants. Although an intracellular cleaved form was observed in the cell lysates, its amount did not change after DMXAA stimulation. These results indicate that STING activates the post-translational processing of SEMA4D on cell surface to release the soluble ectodomain.

Disease-associated mutant of STING induces SEMA4D shedding

Several autosomal dominant mutations of STING have been reported in patients with autoinflammatory diseases (27,28). These mutations encode an active form of STING protein that triggers IRF3-dependent gene induction at steady state. However, a recent study uncovered that IRF3 is dispensable for development of systemic inflammation caused by the disease-associated mutant of STING in mice (22). Therefore, it is possible that the shedding of SEMA4D might be involved in inflammation caused by this STING mutant. To test whether the STING mutant can induce SEMA4D shedding, we established stable cell lines that lack endogenous STING but inducibly expresses WT or the corresponding disease-associated mutant of mouse STING (V146L). After treatment with doxycycline, STING V146L mutant but not STING WT was accumulated in the perinuclear region, where most of them were co-localized with a cis-Golgi matrix protein GM130 (Fig. 4A). We also observed phosphorylation of TBK1 in cells expressing STING V146L but not STING WT (Fig. 4B), confirming the constitutive activation of this STING mutant. Then, we collected the culture supernatants and found that release of soluble SEMA4D was provoked by the expression of the STING mutant.

Thus, SEMA4D shedding is an additional phenotype induced by the disease-associated mutant of STING.

ADAM17 but not TBK1 is required for SEMA4D shedding

Because the active mutant STING that was constitutively localized to the Golgi apparatus was able to induce SEMA4D shedding, STING trafficking may regulate its shedding machinery. As shown in Fig. 5A, treatment of a pharmacological inhibitor brefeldin A (BFA) which inhibits anterograde transport from the ER to Golgi apparatus completely blocked DMXAA-induced release of CXCL10, TNF-α and SEMA4D, suggesting that Golgi apparatus acts as a platform for the induction of all downstream signaling events of STING. It should be noted that BFA also seemed to block SEMA4D trafficking to the plasma membrane, as the smear bands of SEMA4D faster migrated in BFA-treated cells, which may imply incomplete glycosylation or degradation in ER. After translocation to the Golgi apparatus, STING associates with TBK1, triggering CXCL10 and TNF-α gene induction by phosphorylation of IRF3 and NF-κB, respectively (29). Surprisingly, DMXAA-induced SEMA4D shedding was not blocked by BX795, a specific TBK1 inhibitor although it inhibited the induction of CXCL10 (Fig. 5A), indicating that SEMA4D shedding is TBK1-independent. Blocking of NF-κB-dependent transcription by BX795 partially not completely inhibited the release of TNF-α, further supporting the idea that STING promotes its production through a transcription-independent pathway. In addition to SEMA4D, our proteomic analysis revealed that TNF-α, SDC4, TGFBR1 and SORL1 were also released into extracellular space by STING activation (Table 1 and Table S1). All of them are plasma membrane proteins which commonly undergo proteolytic cleavage by ADAM17 (30-32). Therefore, we tested the possibility that ADAM17 is required for STING-mediated SEMA4D release. Inhibition of ADAM17 sheddase activity by a pharmacological inhibitor TMI-1 abolished DMXAA-induced release of TNF-α and SEMA4D but not CXCL10 (Fig. 5A). We also confirmed that TMI-1 inhibited the SEMA4D shedding induced by the active mutant of STING without affecting TBK1 phosphorylation (Fig. 5B). These results suggest that STING activates two independent downstream signaling pathways after trafficking to the Golgi; one is TBK1-mediated gene induction and another is ADAM17-mediated cleavage of plasma membrane proteins (Fig. 5C).

Discussion

In this study, we identified novel STING-dependent signaling in which a cell surface protein SEMA4D is cleaved to produce its soluble ectodomain. The increased concentration of soluble SEMA4D in serum or plasma is associated with numerous inflammatory conditions in humans and mice (26), and the soluble SEMA4D has been described as a stimulator of both innate and acquired immunity (26). STING-dependent polyarthritis in DNaseII-null mice is triggered by innate immune response producing proinflammatory cytokines including TNF-α, IL-6 and IL-1β but not acquired immunity (8). In this case, soluble SEMA4D may contribute to such cytokine production rather than acquired immunity. Indeed, when $CD14^+$ monocytes from rheumatoid arthritis (RA) patients were treated with recombinant soluble SEMA4D protein, the cells produced high levels of TNF-α and IL-6 through a poorly understood mechanism, although its receptor CD72 has been

implicated (33). Furthermore, administration of anti-SEMA4D antibodies to mice with collagen-induced arthritis significantly reduced arthritis score and serum level of TNF-α and IL-6 (33). Thus, the soluble SEMA4D released from STING-activated cells may induce production of inflammatory cytokines in adjacent cells or themselves in a paracrine or autocrine manner.

It has been reported that membrane SEMA4D is cleaved by several proteinases including ADAM17, MT1-MMP and ATAMTS4 (26). Because the potent ADAM17 inhibitor TMI-1 used in this study also inhibits matrix metalloproteinases (MMPs) (34), we could not exclude the possibility that certain MMPs are involved in the STING-mediated SEMA4D shedding. However, our secretome analysis showed that other ADAM17 substrates such as TNF-α, SDC4, TGFBR1 and SORL1 were also released into culture supernatant by STING activation, suggesting that STING activates ADAM17 to promote shedding of these plasma membrane proteins in a cell-intrinsic manner. Although STING is known to activate NF-κB to induce TNF-α gene expression, its activation is very weak compared to IRF3-mediated IFN-β or CXCL10 gene activation (11,23,24). This is supported by our gene expression experiment shown in Fig. 2A. However, the protein level of TNF-α in cell medium was dramatically increased by DMXAA stimulation compared to the mRNA level (Fig. 1C). From these observations, we propose the model that STING activates both transcriptional and post-translational machineries for efficient release of TNF-α. This two-step mechanism comprising NF-κB-mediated TNF-α mRNA induction followed by ADAM17-mediated ectodomain shedding is analogous to the case of another inflammatory cytokine IL-1β whose release is mediated by NF-κB-dependent transcription and caspase-1-dependent proteolytic processing.

How does STING activate ADAM17-dependent shedding machinery? Since the STING mutant that constitutively localized to the Golgi induced ADAM17-mediated shedding of SEMA4D (Fig. 4 and Fig. 5B), STING trafficking from the ER to the Golgi may causes activation of ADAM17. STING activates TBK1 at the Golgi (20), however, inhibition of TBK1 activity by BX795 did not suppress the release of SEMA4D, suggesting involvement of another downstream signaling. Although BX795 partially blocked the release of TNF-α, this discrepancy may be explained by suppression of its transcriptional activation. The enzymatic activity of ADAM17 is tightly regulated by iRhom2-mediated its maturation, localization and conformation (35-39). Upon binding to iRhom2, pro-ADAM17 is exported from the ER to the Golgi, where pro-protein convertases such as Furin cleave auto-inhibitory pro-domain of ADAM17 to be mature form. The interaction with iRhom2 is also required for post-Golgi trafficking of mature ADAM17 to the plasma membrane, and regulates its conformation and proteolytic activity at the cell surface. Interestingly, a recent report shows that iRhom2 directly interacts with STING and mediates its trafficking from the ER to the Golgi (40). In other words, activation of STING induces enrichment of iRhom2 in the Golgi apparatus that may promote ER-Golgi or post-Golgi trafficking of ADAM17. Alternatively, MAPK-mediated regulation might be involved. The activity of ADAM17 has been proposed to be regulated by phosphorylation of ADAM17 and iRhom2 by either ERK or p38 (38, 39, 41-43). Importantly, STING agonists induce MAPK activation independent of

TBK1 whose biological significance has remained unclear (29).

In addition to membrane proteins cleaved by ADAM17, our comprehensive proteomic approach identified Fam3C and LRPAP1 as an intracellular protein secreted from STING-activated cells. Fam3C was originally identified as the interleukin-like epithelial-to-mesenchymal transition (EMT) inducer (ILEI) that is essential for EMT and tumor metastasis (44). Inflammatory injury triggers EMT to promote tissue-remodeling and the sustained EMT causes pathologic fibrosis (45). It would be interesting whether Fam3C is involved in tissue repair or fibrosis during STING-dependent inflammation. LRPAP1, also known as RAP, interacts with members of the LDL receptor family such as LRP1 within the ER to assist the folding of such receptor proteins (46). Because of its high affinity binding, recombinant LRPAP1 protein is used for LRP1 ligand and induces proinflammatory cytokine expression (47). However, whether ER chaperone protein LRPAP1 is secreted in physiological condition was unclear. This is the first evidence that LRPAP1 is secreted in response to inflammatory stimuli.

So far, most studies have focused on IRF3-dependent transcriptional program in the STING pathway, thus no one could find release of SEMA4D, Fam3C and LRPAP1, whose gene expression levels are not altered during STING activation (Fig. 3A). This study provides new insight into the STING-associated inflammatory response and diseases.

Experimental procedures

Reagents

Anti-SEMA4D mAb (#547406) and biotinylated anti-CXCL10 polyAb were purchased from R&D systems (Minneapolis, MN). Anti-α-Tubulin mAb (DM1A) and anti-Flag polyAb were from Sigma-Aldrich (St. Louis, MO). Anti-phospho-TBK1 (Ser172) mAb (D52C2) and anti-TNF-α mAb (D2D4) were from Cell Signalling (Danvers MA). Anti-STING polyAb was from Proteintech (Chicago, IL). Anti-GM130 mAb (35/GM130) was from BD Biosciences (Franklin Lakes, NJ). DMXAA was from Ark Pharm, Inc (Arlington Heights, IL). Doxycycline was from Wako Pure Chemical Industries, Ltd (Osaka, Japan). BFA was from Cayman Chemical (Ann Arbor, MI). BX795, TMI-1 and CHX were from Sigma-Aldrich.

Cell lines

Raw264.7 cells were cultured in DMEM containing 10% FCS. The CRISPR/Cas9-mediated gene editing was used to establish Raw264.7 cells lacking STING. Px330 vector expressing Cas9 and sgRNA for mouse STING (16) was transfected into Raw264.7 cells by electroporation using the NEPA21 system (135V, 10ms; Nepagene, Chiba, Japan). After 24-h incubation at 37 ºC, the cells were subjected to limiting dilution, and the mutated clones were identified by Western blotting. For rescue experiment, the C-terminal Flag-tagged mouse STING (STING-Flag) was stably expressed in STING deficient cells using the PiggyBac transposon system. To generate the inducible gene expression cells, Tet-on expression vector carrying STING-Flag WT or V146L mutant was introduced into the STING deficient cells. The V146L mutant STING was constructed with recombinant PCR using primers of 5'-CACCGGCCAGTGTGGTGGAAGATGCCATACTC CAACCT-3' (BstXI-Start) and 5'-CAGCGGAAGTCTCTGCACTCTGTGAAGAAAA

GAAGTT-3' (V146L), and 5'-AACTTCTTTTCTTCACAGAGTGCAGAGACTTCCGCTG-3' (V146L) and 5'-GCTAACCACTGTGCTGGCTACTTATCGTCGTCATCCTTGTAATCGATGAGGTCAGTGCGGAGTG-3' (Flag-Stop-BstXI).

Sample preparation for secretome analysis

Raw264.7 cells were seeded in 6-well plates (2.5×10^6 cells/well) and cultured overnight. After washing with PBS twice, the cells were cultured with FCS-free DMEM medium containing DMSO or 100 μg/ml DMXAA for 4 h. The conditioned medium was collected and centrifuged at 400 g for 10 min at 4 ºC. The supernatants were concentrated to 100 μl using Amicon Ultra 3K filter (Millipore, Burlington, MA) and proteins were purified by methanol/chloroform precipitation. The protein pellets were solubilized in 20 μl of 8 M urea, followed by reduction in 5 mM DTT at 37 ºC for 30 min and alkylation in 27.5 mM IAA at room temperature for 30 min in the dark. After reducing the urea concentration to 1 M with 50 mM Tris-HCl (pH8.0), the proteins were digested with 50 ng Trypsin/Lys-C Mix, Mass Spec Grade (Promega, Madison, WI) at 37 ºC overnight. The peptides were desalted using GL-Tip SDB (GL Sciences, Tokyo, Japan) according to the manufacturer's protocol and the eluates were evaporated in a Speed Vac Concentrator (Thermo Fisher Scientific, Waltham, MA). The residues were dissolved in 0.1% TFA.

Data-dependent LC-MS/MS analysis

LC-MS/MS analysis of the resultant peptides (200 ng each) was performed on an EASY-nLC 1200 UHPLC connected to a Q Exactive Plus mass spectrometer through a nanoelectrospray ion source (Thermo Fisher Scientific). The peptides were separated on a 75 μm inner diameter × 120 mm C18 reversed-phase column (Nikkyo Technos, Tokyo, Japan) with a linear gradient from 4–28% acetonitrile (ACN) for min 0–150 followed by increase to 80% ACN during min 150–170. The mass spectrometer was operated in a data-dependent acquisition mode with a top 10 MS/MS method. Raw data were directly analyzed against the SwissProt database restricted to *M. musculus* using Proteome Discoverer version 2.2 (Thermo Fisher Scientific) for identification and label-free precursor ion quantification. Normalization was performed such that the total sum of abundance values for each sample over all peptides is the same. The mass spectrometry proteomics data have been deposited to the ProteomeXchange Consortium via the jPOST partner repository (https://repository.jpostdb.org) with the dataset identifier PXD009169. The data were analyzed by a two-tailed Student's *t*-test and the resulting *p*-values were adjusted using the Benjamini-Hochberg method for controlling the false discovery rate (FDR). A volcano plot was used for showing the fold changes and *q*-values (FDR corrected *p*-values) of each protein. To select significant proteins, we set fold-change threshold of 4 and *q*-value threshold of 0.05.

PRM analysis

To quantify SEMA4D, LRPAP1, Fam3C, SEMA4B, CCL9, IFN-β, CXCL10, and TNF-α, at least three peptides per protein were measured by PRM, an MS/MS-based targeted quantification method using high-resolution mass spectrometry. Time alignment and relative quantification of the transitions were performed with PinPoint version 1.4 (Thermo Fisher Scientific). The mass spectrometry proteomics data

have been deposited to the ProteomeXchange Consortium via the jPOST partner repository with the dataset identifier PXD009170.

SDS-PAGE and Western blotting

The culture medium was replaced with 0.1% FCS/DMEM when the cells were treated with DMXAA in the presence or absence of inhibitors, and the conditioned media were concentrated by Amicon Ultra 3K filter or Vivaspin 10K filter (Sartorius, Goettingen, Germany). At the same condition, the cells were lysed on ice for 10 min in lysis buffer (20 mM Tris-HCl [pH7.5], 150 mM NaCl, 1 mM EDTA, 1% NP-40, 10% glycerol, a protease inhibitor cocktail [Nacalai Tesque, Kyoto, Japan] and a phosphatase inhibitor cocktail [Nacalai Tesque]) and centrifuged at 20,000 g for 15 min at 4 ºC. The concentrated media or the cell lysates were mixed with 5×SDS sample buffer (200 mM Tris-HCl buffer [pH 6.8], 10% SDS, 25% glycerol, and 0.05% bromophenol blue) with 5% β-mercaptoethanol, and heated at 95°C for 5 min. The samples were separated by electrophoresis on a 6% (for SEMA4D), 10% (for α-Tubulin, phospho-TBK1 and STING) or 16% (for CXCL10 and TNF-α) polyacrylamide gel, transferred onto a PVDF membrane (Millipore). After blocking, the membrane was incubated with primary antibodies in 5% skim milk or in Signal Enhancer HIKARI (Nacalai Tesque) overnight at 4°C, followed by incubation with HRP-conjugated secondary antibodies. Protein bands in the membrane was detected using ImageQuant LAS 4000 mini (GE Healthcare, Little Chalfont, United Kingdom) after incubation of the membrane with Clarity Western ECL Substrate (BIO-RAD, Hercules, CA) or Immunostar LD (Wako Pure Chemical Industries, Ltd).

Real-time PCR

Total RNA was isolated using RNAiso plus (TAKARA, Shiga, Japan) according to the manufacturer's protocol. The RNA was reverse-transcribed using the ReverTra Ace qPCR RT Master Mix (TOYOBO, Osaka, Japan), and real-time PCR was performed with the Light-Cycler 96 (Roche Diagnostics, Basel, Switzerland) using the FastStart Essential DNA Green Master Mix (Roche Diagnostics). The primers used for real-time PCR were as follows: IFN-β, 5′-CCACCACAGCCCTCTCCATCAACTAT-3′ and 5′-CAAGTGGAGAGCAGTTGAGGACATC-3′; CXCL10, 5′-CCATCAGCACCATGAACCCAAGT-3′ and 5′-CACTCCAGTTAAGGAGCCCTTTTAGACC-3′; SEMA4D, 5'-TTGGGCAGTGAACCCATCATC-3' and 5'-GGATCACGTCAGCAAAGACGA-3'; TNF-α, 5'-CACAGAAAGCATGATCCGCGACGT-3' and 5'-CGGCAGAGAGGAGGTTGACTTTCT-3'; β-actin, 5′-TGTGATGGTGGGAATGGGTCAG-3′ and 5′-TTTGATGTCACGCACGATTTCC-3′.

Immunostaining

The STING-null Raw264.7 cells expressing Tet-on-STING-Flag WT or Tet-on-STING-Flag V146L were seeded on coverslips in a 12-well plate. After treatment with doxycycline, the cells were fixed with 3.7% formaldehyde/PBS for 15 min at 37°C and permeabilized with 0.2% Triton X-100/PBS for 10 min at room temperature. The coverslips were incubated with primary antibodies in 2% goat serum/PBS for 1 h at 37°C. After washing with PBS three times, the coverslips were incubated with Alexa Fluor-488 goat anti mouse IgG and Alexa Fluor-555 goat anti rabbit IgG for 1 h at room temperature in the dark. After

washing with PBS three times and subsequent rinse with distilled water, the coverslips were mounted on the glass slides with ProLong Gold Antifade Mountant with DAPI (Thermo Fisher Scientific). The immunofluorescence images were obtained by a confocal laser scanning microscope FV1200 (Olympus, Tokyo, Japan).

Acknowledgments: We thank M. Kajimoto and M. Kawano for technical assistance. We also thank M. Iwata for secretarial assistance.

Conflict of interest: The authors declare that they have no conflicts of interest with the contents of this article.

Author contributions: K.M. designed and performed most experiments. H.K. performed LC-MS/MS analysis. K.M. wrote the paper with H.K.

References

1. Wu, J., and Chen, Z. J. (2014) Innate immune sensing and signaling of cytosolic nucleic acids. *Annu. Rev. Immunol.* **32**, 461-488
2. Ablasser, A., Hertrich, C., Wassermann, R., and Hornung, V. (2013) Nucleic acid driven sterile inflammation. *Clin. Immunol.* **147**, 207-215
3. Nagata, S., Hanayama, R., and Kawane, K. (2010) Autoimmunity and the clearance of dead cells. *Cell* **140**, 619-630
4. Chasis, J. A., and Mohandas, N. (2008) Erythroblastic islands: niches for erythropoiesis. *Blood* **112**, 470-478
5. Kawane, K., Fukuyama, H., Kondoh, G., Takeda, J., Ohsawa, Y., Uchiyama, Y., and Nagata, S. (2001) Requirement of DNase II for definitive erythropoiesis in the mouse fetal liver. *Science* **292**, 1546-1549
6. Kawane, K., Ohtani, M., Miwa, K., Kizawa, T., Kanbara, Y., Yoshioka, Y., Yoshikawa, H., and Nagata, S. (2006) Chronic polyarthritis caused by mammalian DNA that escapes from degradation in macrophages. *Nature* **443**, 998-1002
7. Yoshida, H., Okabe, Y., Kawane, K., Fukuyama, H., and Nagata, S. (2005) Lethal anemia caused by interferon-beta produced in mouse embryos carrying undigested DNA. *Nat. Immunol.* **6**, 49-56
8. Kawane, K., Tanaka, H., Kitahara, Y., Shimaoka, S., and Nagata, S. (2010) Cytokine-dependent but acquired immunity-independent arthritis caused by DNA escaped from degradation. *Proc. Natl. Acad. Sci. U.S.A.* **107**, 19432-19437
9. Kawane, K., Motani, K., and Nagata, S. (2014) DNA degradation and its defects. *Cold Spring Harb. Perspect. Biol.* **6**, a016394
10. Rodero, M. P., Tesser, A., Bartok, E., Rice, G. I., Della Mina, E., Depp, M., Beitz, B., Bondet, V., Cagnard, N., Duffy, D., Dussiot, M., Fremond, M. L., Gattorno, M., Guillem, F., Kitabayashi, N., Porcheray, F., Rieux-Laucat, F., Seabra, L., Uggenti, C., Volpi, S., Zeef, L. A. H., Alyanakian, M. A., Beltrand, J., Bianco, A. M., Boddaert, N., Brouzes, C., Candon, S., Caorsi, R., Charbit, M., Fabre, M., Faletra, F., Girard, M., Harroche, A., Hartmann, E., Lasne, D., Marcuzzi, A., Neven, B., Nitschke, P., Pascreau, T., Pastore, S., Picard, C., Picco, P.,

Piscianz, E., Polak, M., Quartier, P., Rabant, M., Stocco, G., Taddio, A., Uettwiller, F., Valencic, E., Vozzi, D., Hartmann, G., Barchet, W., Hermine, O., Bader-Meunier, B., Tommasini, A., and Crow, Y. J. (2017) Type I interferon-mediated autoinflammation due to DNase II deficiency. *Nat. Commun.* **8**, 2176

11. Ishikawa, H., and Barber, G. N. (2008) STING is an endoplasmic reticulum adaptor that facilitates innate immune signalling. *Nature* **455**, 674-678
12. Sun, L., Wu, J., Du, F., Chen, X., and Chen, Z. J. (2013) Cyclic GMP-AMP synthase is a cytosolic DNA sensor that activates the type I interferon pathway. *Science* **339**, 786-791
13. Wu, J., Sun, L., Chen, X., Du, F., Shi, H., Chen, C., and Chen, Z. J. (2013) Cyclic GMP-AMP is an endogenous second messenger in innate immune signaling by cytosolic DNA. *Science* **339**, 826-830
14. Gao, P., Ascano, M., Wu, Y., Barchet, W., Gaffney, B. L., Zillinger, T., Serganov, A. A., Liu, Y., Jones, R. A., Hartmann, G., Tuschl, T., and Patel, D. J. (2013) Cyclic [G(2',5')pA(3',5')p] is the metazoan second messenger produced by DNA-activated cyclic GMP-AMP synthase. *Cell* **153**, 1094-1107
15. Gao, P., Ascano, M., Zillinger, T., Wang, W., Dai, P., Serganov, A. A., Gaffney, B. L., Shuman, S., Jones, R. A., Deng, L., Hartmann, G., Barchet, W., Tuschl, T., and Patel, D. J. (2013) Structure-function analysis of STING activation by c[G(2',5')pA(3',5')p] and targeting by antiviral DMXAA. *Cell* **154**, 748-762
16. Motani, K., Ito, S., and Nagata, S. (2015) DNA-Mediated Cyclic GMP-AMP Synthase-Dependent and -Independent Regulation of Innate Immune Responses. *J. Immunol.* **194**, 4914-4923
17. Saitoh, T., Fujita, N., Hayashi, T., Takahara, K., Satoh, T., Lee, H., Matsunaga, K., Kageyama, S., Omori, H., Noda, T., Yamamoto, N., Kawai, T., Ishii, K., Takeuchi, O., Yoshimori, T., and Akira, S. (2009) Atg9a controls dsDNA-driven dynamic translocation of STING and the innate immune response. *Proc. Natl. Acad. Sci. U.S.A.* **106**, 20842-20846
18. Ishikawa, H., Ma, Z., and Barber, G. N. (2009) STING regulates intracellular DNA-mediated, type I interferon-dependent innate immunity. *Nature* **461**, 788-792
19. Tanaka, Y., and Chen, Z. J. (2012) STING specifies IRF3 phosphorylation by TBK1 in the cytosolic DNA signaling pathway. *Sci. Signal.* **5**, ra20

20. Mukai, K., Konno, H., Akiba, T., Uemura, T., Waguri, S., Kobayashi, T., Barber, G. N., Arai, H., and Taguchi, T. (2016) Activation of STING requires palmitoylation at the Golgi. *Nat. Commun.* **7**, 11932

21. Okabe, Y., Kawane, K., and Nagata, S. (2008) IFN regulatory factor (IRF) 3/7-dependent and -independent gene induction by mammalian DNA that escapes degradation. *Eur. J. Immunol.* **38**, 3150-3158

22. Warner, J. D., Irizarry-Caro, R. A., Bennion, B. G., Ai, T. L., Smith, A. M., Miner, C. A., Sakai, T., Gonugunta, V. K., Wu, J., Platt, D. J., Yan, N., and Miner, J. J. (2017) STING-associated vasculopathy develops independently of IRF3 in mice. *J. Exp. Med.* **214**, 3279-3292

23. Roberts, Z. J., Goutagny, N., Perera, P. Y., Kato, H., Kumar, H., Kawai, T., Akira, S., Savan, R., van Echo, D., Fitzgerald, K. A., Young, H. A., Ching, L. M., and Vogel, S. N. (2007) The chemotherapeutic agent DMXAA potently and specifically activates the TBK1-IRF-3 signaling axis. *J. Exp. Med.* **204**, 1559-1569

24. Prantner, D., Perkins, D. J., Lai, W., Williams, M. S., Sharma, S., Fitzgerald, K. A., and Vogel, S. N. (2012) 5,6-Dimethylxanthenone-4-acetic acid (DMXAA) activates stimulator of interferon gene (STING)-dependent innate immune pathways and is regulated by mitochondrial membrane potential. *J. Biol. Chem.* **287**, 39776-39788

25. Rauniyar, N. (2015) Parallel Reaction Monitoring: A Targeted Experiment Performed Using High Resolution and High Mass Accuracy Mass Spectrometry. *Int. J. Mol. Sci.* **16**, 28566-28581

26. Maleki, K. T., Cornillet, M., and Bjorkstrom, N. K. (2016) Soluble SEMA4D/CD100: A novel immunoregulator in infectious and inflammatory diseases. *Clin. Immunol.* **163**, 52-59

27. Liu, Y., Jesus, A. A., Marrero, B., Yang, D., Ramsey, S. E., Sanchez, G. A. M., Tenbrock, K., Wittkowski, H., Jones, O. Y., Kuehn, H. S., Lee, C. R., DiMattia, M. A., Cowen, E. W., Gonzalez, B., Palmer, I., DiGiovanna, J. J., Biancotto, A., Kim, H., Tsai, W. L., Trier, A. M., Huang, Y., Stone, D. L., Hill, S., Kim, H. J., Hilaire, C. S., Gurprasad, S., Plass, N., Chapelle, D., Horkayne-Szakaly, I., Foell, D., Barysenka, A., Candotti, F., Holland, S. M., Hughes, J. D., Mehmet, H., Issekutz, A. C., Raffeld, M., McElwee, J., Fontana, J. R., Minniti, C. P., Moir, S., Kastner, D. L., Gadina, M., Steven, A. C., Wingfield, P. T., Brooks, S. R., Rosenzweig, S.

D., Fleisher, T. A., Deng, Z., Boehm, M., Paller, A. S., and Goldbach-Mansky, R. (2014) Activated STING in a vascular and pulmonary syndrome. *N. Engl. J. Med.* **371**, 507-518

28. Jeremiah, N., Neven, B., Gentili, M., Callebaut, I., Maschalidi, S., Stolzenberg, M. C., Goudin, N., Fremond, M. L., Nitschke, P., Molina, T. J., Blanche, S., Picard, C., Rice, G. I., Crow, Y. J., Manel, N., Fischer, A., Bader-Meunier, B., and Rieux-Laucat, F. (2014) Inherited STING-activating mutation underlies a familial inflammatory syndrome with lupus-like manifestations. *J. Clin. Invest.* **124**, 5516-5520

29. Abe, T., and Barber, G. N. (2014) Cytosolic-DNA-mediated, STING-dependent proinflammatory gene induction necessitates canonical NF-kappaB activation through TBK1. *J. Virol.* **88**, 5328-5341

30. Dreymueller, D., Pruessmeyer, J., Groth, E., and Ludwig, A. (2012) The role of ADAM-mediated shedding in vascular biology. *Eur. J. Cell Biol.* **91**, 472-485

31. Liu, C., Xu, P., Lamouille, S., Xu, J., and Derynck, R. (2009) TACE-mediated ectodomain shedding of the type I TGF-beta receptor downregulates TGF-beta signaling. *Mol. Cell* **35**, 26-36

32. Tsukamoto, S., Takeuchi, M., Kawaguchi, T., Togasaki, E., Yamazaki, A., Sugita, Y., Muto, T., Sakai, S., Takeda, Y., Ohwada, C., Sakaida, E., Shimizu, N., Nishii, K., Jiang, M., Yokote, K., Bujo, H., and Nakaseko, C. (2014) Tetraspanin CD9 modulates ADAM17-mediated shedding of LR11 in leukocytes. *Exp. Mol. Med.* **46**, e89

33. Yoshida, Y., Ogata, A., Kang, S., Ebina, K., Shi, K., Nojima, S., Kimura, T., Ito, D., Morimoto, K., Nishide, M., Hosokawa, T., Hirano, T., Shima, Y., Narazaki, M., Tsuboi, H., Saeki, Y., Tomita, T., Tanaka, T., and Kumanogoh, A. (2015) Semaphorin 4D Contributes to Rheumatoid Arthritis by Inducing Inflammatory Cytokine Production: Pathogenic and Therapeutic Implications. *Arthritis Rheum.* **67**, 1481-1490

34. Moss, M. L., and Rasmussen, F. H. (2007) Fluorescent substrates for the proteinases ADAM17, ADAM10, ADAM8, and ADAM12 useful for high-throughput inhibitor screening. *Anal. Biochem.* **366**, 144-148

35. Adrain, C., Zettl, M., Christova, Y., Taylor, N., and Freeman, M. (2012) Tumor necrosis factor signaling requires iRhom2 to promote trafficking and activation of TACE. *Science* **335**, 225-228

36. McIlwain, D. R., Lang, P. A., Maretzky, T., Hamada, K., Ohishi, K., Maney, S. K., Berger, T., Murthy, A., Duncan, G., Xu, H. C., Lang, K. S., Haussinger, D., Wakeham, A., Itie-Youten, A., Khokha, R., Ohashi, P. S., Blobel, C. P., and Mak, T. W. (2012) iRhom2 regulation of TACE controls TNF-mediated protection against Listeria and responses to LPS. *Science* **335**, 229-232

37. Brooke, M. A., Etheridge, S. L., Kaplan, N., Simpson, C., O'Toole, E. A., Ishida-Yamamoto, A., Marches, O., Getsios, S., and Kelsell, D. P. (2014) iRHOM2-dependent regulation of ADAM17 in cutaneous disease and epidermal barrier function. *Hum. Mol. Genet.* **23**, 4064-4076

38. Grieve, A. G., Xu, H., Kunzel, U., Bambrough, P., Sieber, B., and Freeman, M. (2017) Phosphorylation of iRhom2 at the plasma membrane controls mammalian TACE-dependent inflammatory and growth factor signalling. *Elife* **6**, e23968

39. Cavadas, M., Oikonomidi, I., Gaspar, C. J., Burbridge, E., Badenes, M., Felix, I., Bolado, A., Hu, T., Bileck, A., Gerner, C., Domingos, P. M., von Kriegsheim, A., and Adrain, C. (2017) Phosphorylation of iRhom2 Controls Stimulated Proteolytic Shedding by the Metalloprotease ADAM17/TACE. *Cell Rep.* **21**, 745-757

40. Luo, W. W., Li, S., Li, C., Lian, H., Yang, Q., Zhong, B., and Shu, H. B. (2016) iRhom2 is essential for innate immunity to DNA viruses by mediating trafficking and stability of the adaptor STING. *Nat. Immunol.* **17**, 1057-1066

41. Soond, S. M., Everson, B., Riches, D. W., and Murphy, G. (2005) ERK-mediated phosphorylation of Thr735 in TNFalpha-converting enzyme and its potential role in TACE protein trafficking. *J. Cell Sci.* **118**, 2371-2380

42. Xu, P., and Derynck, R. (2010) Direct activation of TACE-mediated ectodomain shedding by p38 MAP kinase regulates EGF receptor-dependent cell proliferation. *Mol. Cell* **37**, 551-566

43. Xu, P., Liu, J., Sakaki-Yumoto, M., and Derynck, R. (2012) TACE activation by MAPK-mediated regulation of cell surface dimerization and TIMP3 association. *Sci. Signal.* **5**, ra34

44. Waerner, T., Alacakaptan, M., Tamir, I., Oberauer, R., Gal, A., Brabletz, T., Schreiber, M., Jechlinger, M., and Beug, H. (2006) ILEI: a cytokine essential for EMT, tumor formation, and late events in metastasis in epithelial cells. *Cancer Cell* **10**, 227-239

45. Stone, R. C., Pastar, I., Ojeh, N., Chen, V., Liu, S., Garzon, K. I., and Tomic-Canic, M. (2016)

Epithelial-mesenchymal transition in tissue repair and fibrosis. *Cell Tissue Res.* **365**, 495-506

46. Bu, G., and Rennke, S. (1996) Receptor-associated protein is a folding chaperone for low density lipoprotein receptor-related protein. *J. Biol. Chem.* **271**, 22218-22224

47. Brifault, C., Gilder, A. S., Laudati, E., Banki, M., and Gonias, S. L. (2017) Shedding of membrane-associated LDL receptor-related protein-1 from microglia amplifies and sustains neuroinflammation. *J. Biol. Chem.* **292**, 18699-18712

FOOTNOTES

This work was supported by the JSPS KAKENHI (Grant Numbers 15K19024 and 17K08661) and the Takeda Science Foundation (to K.M.), and by the JSPS KAKENHI (Grand Number 17K08635) and the Japan Foundation for Applied Enzymology (to H.K.).

The abbreviations used are: STING, stimulator of interferon genes; ER, endoplasmic reticulum; TBK1, TANK-binding kinase 1; SEMA4D, semaphorin-4D; ADAM17, a disintegrin and metalloproteinase 17; cGAMP, cyclic GMP-AMP; cGAS, cGAMP synthase; IFN, interferon; ISG, IFN-stimulated genes; CHX, cycloheximide; DMXAA, 5, 6-dimethylxanthenone-4-acetic acid; PSM, peptide spectrum match; BFA, brefeldin A

Table 1

The proteins increased by DMXAA stimulation on the secretome analysis.

More than 4-fold and significantly ($q < 0.05$) increased proteins were listed.

Gene Symbol	Description	# PSMs	# Peptides	Coverage [%]	Fold increase (DMXAA/DMSO)
Ccl4	C-C motif chemokine 4	914	6	55	80.1
Tnf	Tumor necrosis factor	424	13	58	141.9
Glg1	Golgi apparatus protein 1	264	42	45	9.4
Sema4d	Semaphorin-4D	218	20	31	4.3
Sdc4	Syndecan-4	168	5	22	22.3
Mthfd1	C-1-tetrahydrofolate synthase, cytoplasmic	140	28	41	5.0
H2-T23	H-2 class I histocompatibility antigen, D-37 alpha chain	55	3	19	5.6
Cxcl10	C-X-C motif chemokine 10	45	5	34	94.2
Ccl2	C-C motif chemokine 2	45	4	21	8.4
Fam3c	Protein FAM3C	36	5	26	6.6
Hist1h1d	Histone H1.3	25	1	26	5.0
Tor3a	Torsin-3A	23	5	18	6.0
Ifnb1	Interferon beta	18	4	18	28.0
Lrpap1	Alpha-2-macroglobulin receptor-associated protein	14	4	12	5.9
Cxcl2	C-X-C motif chemokine 2	13	2	36	18.9
Ccl5	C-C motif chemokine 5	7	2	21	41.9
Icam2	Intercellular adhesion molecule 2	7	2	6	4.8
Golim4	Golgi integral membrane protein 4	6	4	10	4.2
Acvr1	Activin receptor type-1	6	1	2	6.4
Lif	Leukemia inhibitory factor	5	1	5	8.3
Ube2d3	Ubiquitin-conjugating enzyme E2 D3	4	2	29	19.7
Qsox2	Sulfhydryl oxidase 2	4	3	6	4.4
Lrig2	Leucine-rich repeats and immunoglobulin-like domains protein 2	1	1	2	4.7

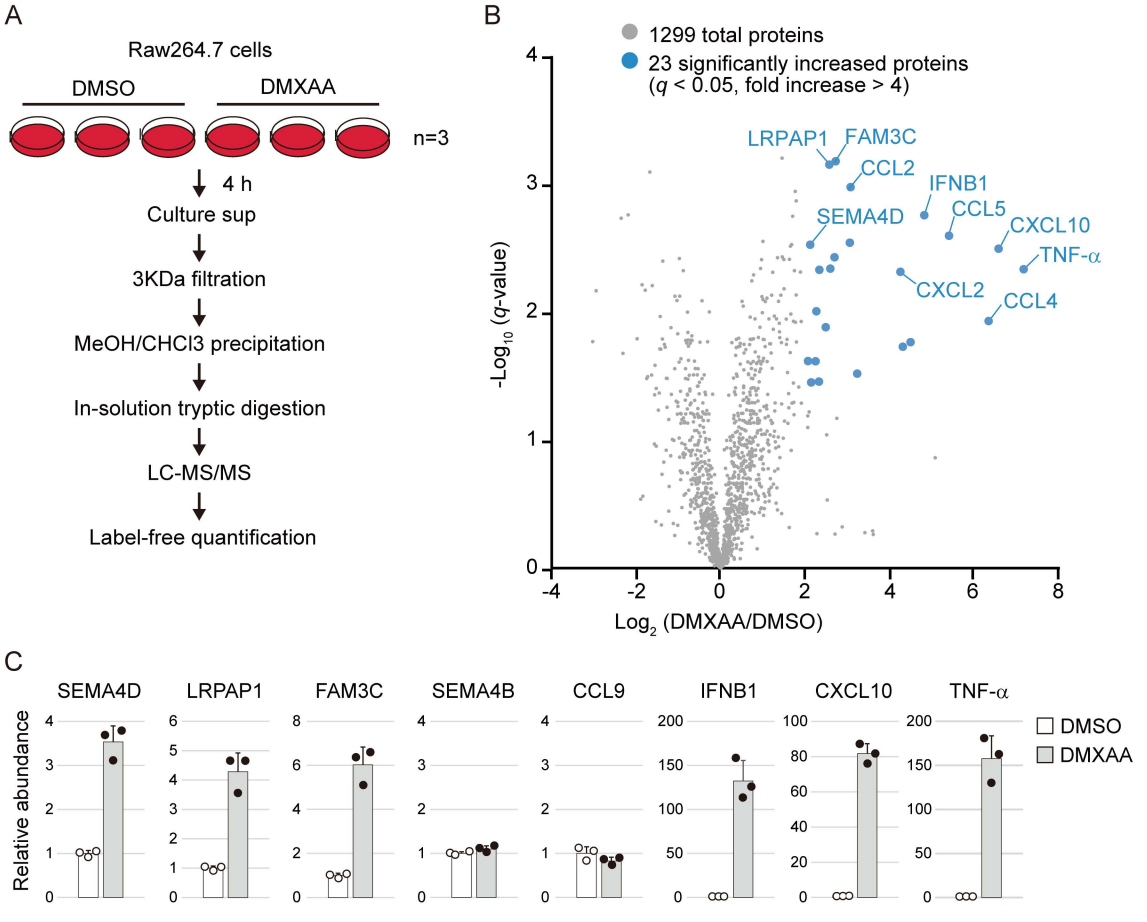

Figure 1. Secretome analysis of DMXAA-treated cells. *A*, A schematic diagram of the label-free quantitative proteomics workflow. Raw264.7 cells were cultured in serum-free DMEM containing DMSO or 100 μg/ml DMXAA for 4 h, and the conditioned medium was collected. The precipitated proteins were directly digested with trypsin/Lys-C. Three biological replicates for each sample were individually prepared and analyzed by LC-MS/MS. Label-free quantification was performed using Proteome Discoverer 2.2 software. *B*, Volcano plot showing differential protein profiles in DMSO- and DMXAA-treated cell culture medium. The X-axis indicates log2 fold-change upon DMXAA-stimulation. The Y-axis indicates negative log10 of the *t*-test *q*-value. More than 4-fold increased proteins with statistical significance ($q < 0.05$) are shown by blue circles. *C*, Accurate amount of protein in the samples used for proteomics was measured by target LC-MS/MS using the PRM method. The relative abundance was calculated as compared to DMSO control. Scatter plots show the individual data and bar graphs indicate mean ± SD (n=3).

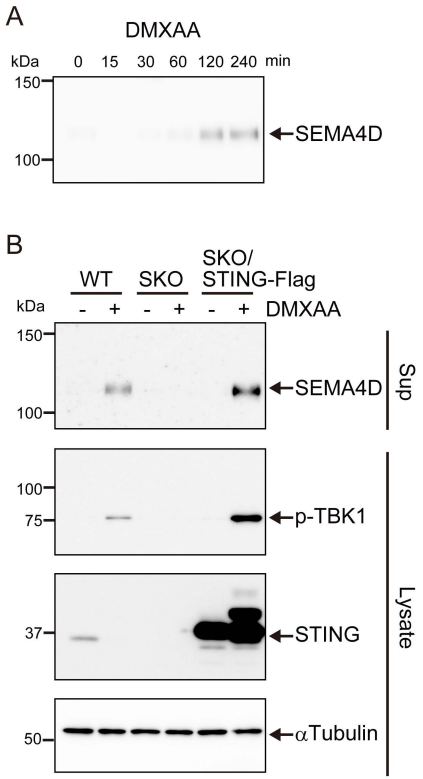

Figure 2. STING-dependent release of SEMA4D. *A*, Raw264.7 cells were cultured in 0.1% FCS/DMEM containing 100 μg/ml DMXAA for 0, 15, 30, 60, 120 and 240 min. Soluble SEMA4D in the culture supernatants was detected by Western blotting with anti-SEMA4D antibody. *B*, WT, STING$^{-/-}$ (SKO), and STING$^{-/-}$ Raw264.7 cells ectopically expressing STING-Flag (SKO/STING-Flag) were cultured in 0.1% FCS/DMEM containing DMSO (-) or 100 μg/ml DMXAA for 4 h. The culture supernatants and the cell lysates were analyzed by Western blotting with anti-SEMA4D, anti-phospho-TBK1, anti-STING, or anti-α-Tubulin.

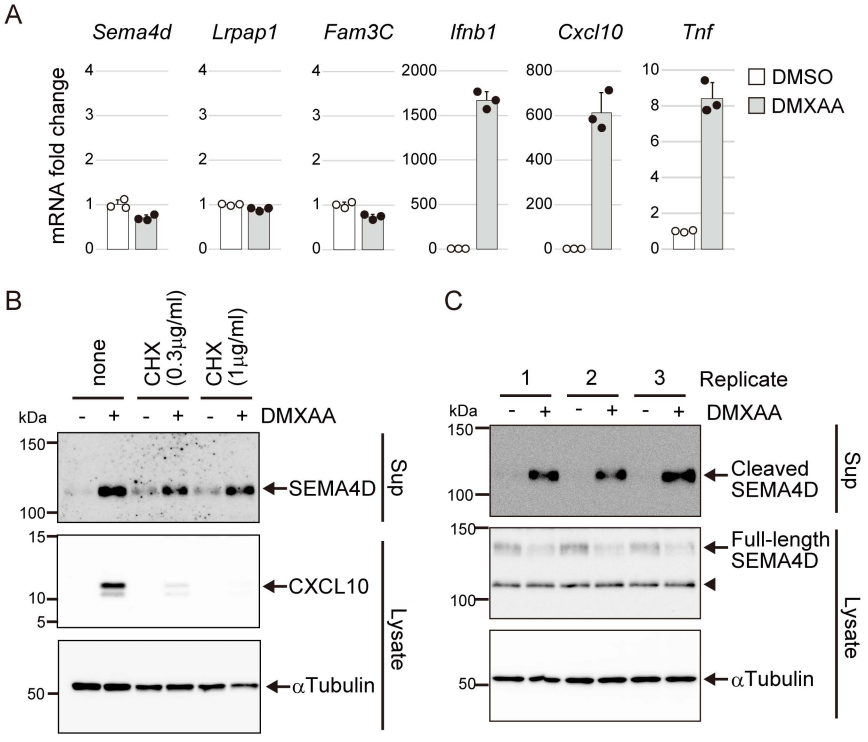

Figure 3. Activation of STING induces shedding of SEMA4D in a transcription-independent manner. *A* and *C*, Raw264.7 cells were cultured in 0.1% FCS/DMEM containing DMSO (-) or 100 μg/ml DMXAA for 4 h. In *A*, the mRNA levels of indicated genes were determined by real-time PCR. The data are normalized by β-actin mRNA and shown as fold change relative to DMSO control. Scatter plots show the individual data and bar graphs indicate mean ± SD (n=3). *B*, Raw264.7 cells were cultured in 0.1% FCS/DMEM with or without indicated concentrations of CHX for 30 min and then further incubated with DMSO (-) or 100 μg/ml DMXAA for 4 h. SEMA4D and CXCL10 levels in culture supernatants and α-Tubulin level in cell lysates were determined by Western blotting with anti-SEMA4D, anti-CXCL10 and anti-α-Tubulin. In *C*, protein levels of soluble SEMA4D in culture supernatants and membrane SEMA4D in cell lysates from three biological replicates were analyzed by Western blotting with anti-SEMA4D. Arrowhead indicates an intracellular cleaved form of SEMA4D.

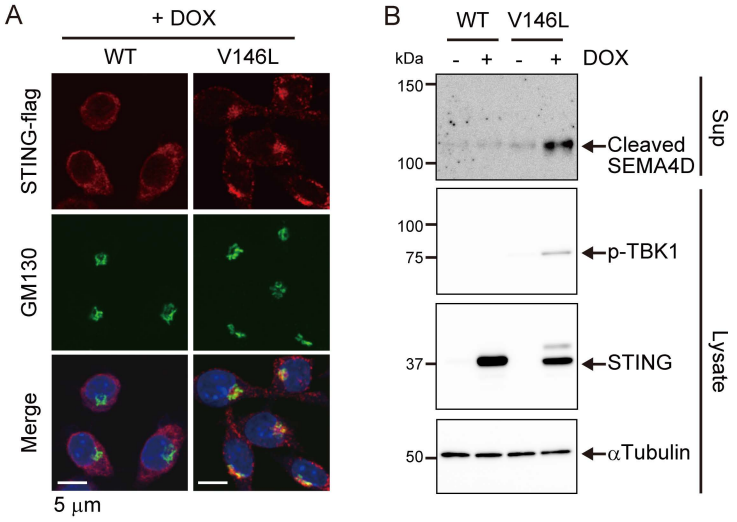

Figure 4. Disease-associated mutant of STING activates SEMA4D shedding. *A* and *B*, STING$^{-/-}$ Raw264.7 cells expressing the Tet-on-STING-Flag wild-type (WT) or Tet-on-STING-Flag V146L mutant (V146L) were cultured in 0.1% FCS/DMEM with or without 1 μg/ml doxycycline (DOX) for 4 h. In *A*, the cells were fixed and co-stained with anti-Flag and anti-GM130 antibodies, followed by examination under conforcal microscopy. Scale bars, 5 μm. In *B*, the culture supernatants and the cell lysates were analyzed by Western blotting with anti-SEMA4D, anti-phospho-TBK1, anti-STING, or anti-α-Tubulin.

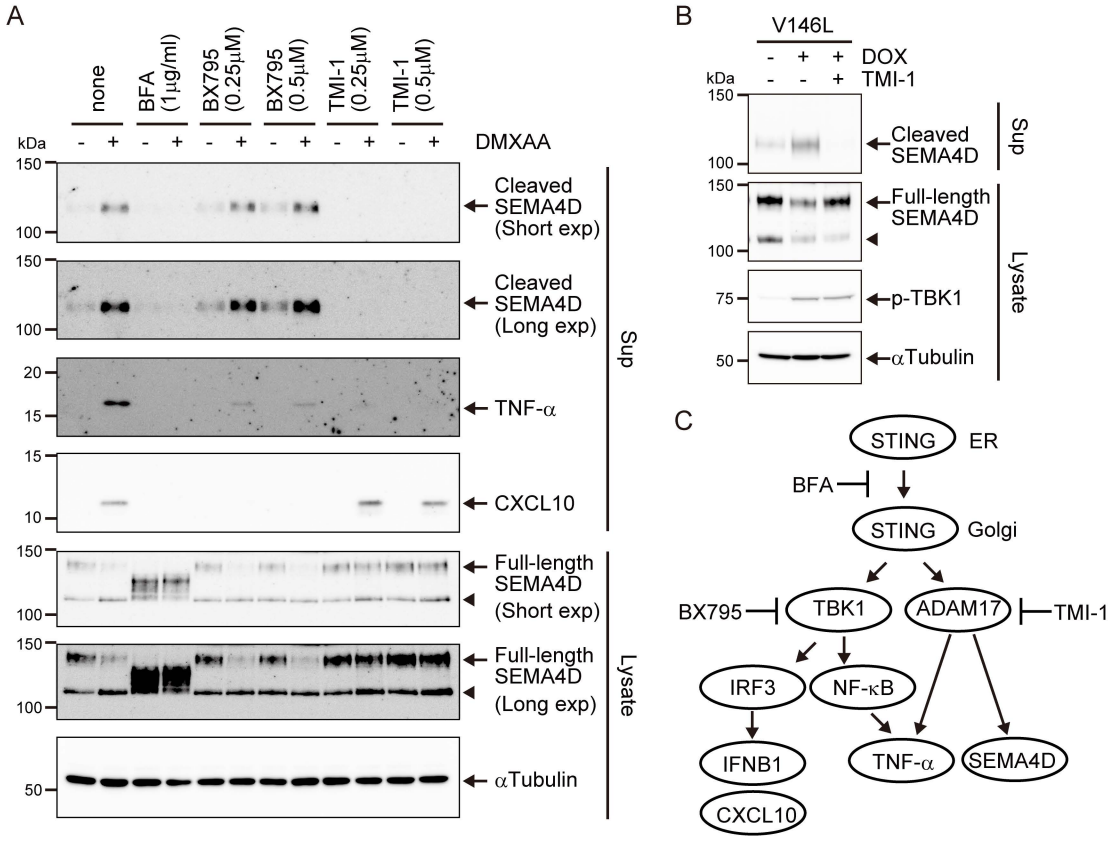

Figure 5. ADAM17 but not TBK1 activity is required for STING-dependent SEMA4D shedding. *A*, Raw264.7 cells were cultured in 0.1% FCS/DMEM with or without indicated inhibitors for 30 min and then further incubated with DMSO (-) or 100 μg/ml DMXAA for 4 h. Indicated protein levels in culture supernatants and cell lysates were determined by Western blotting with anti-SEMA4D, anti-TNF-α, anti-CXCL10 and anti-α-Tubulin. *B*, STING$^{-/-}$ Raw264.7 cells expressing the Tet-on-STING-Flag V146L mutant (V146L) were cultured in 0.1% FCS/DMEM with or without TMI-1 (0.5 μM) for 30 min and then further incubated with or without 1 μg/ml doxycycline (DOX) for 4 h. The culture supernatants and the cell lysates were analyzed by Western blotting with anti-SEMA4D, anti-phospho-TBK1 or anti-α-Tubulin. *C*, A proposed model of the STING-mediated inflammatory signaling pathways. Once STING is activated by agonist or genetic mutation, it relocates from the ER to the Golgi apparatus, which induces ADAM17-mediated post-translational shedding pathway independent of TBK1-mediated transcriptional pathway. This ectodomain shedding is required for producing biologically active inflammatory proteins such as SEMA4D and TNF-α. Arrowheads indicate an intracellular cleaved form of SEMA4D.

Activation of stimulator of interferon genes (STING) induces ADAM17-mediated shedding of the immune semaphorin SEMA4D

Kou Motani and Hidetaka Kosako

J. Biol. Chem. published online April 4, 2018
